

phys. stat. sol. (a) **57**, 179 (1980)

Subject classification: 18.2; 18.4; 22.8

IV. Physikalisches Institut der Universität Göttingen

Double Exchange in $\text{Cr}_x\text{Mn}_{1-x}\text{As}$ Compounds¹⁾

By

R. WÖHL, H. BERG²⁾, and K. BÄRNER

The magnetic moment M and the specific resistivity ρ of $\text{Cr}_x\text{Mn}_{1-x}\text{As}$ polycrystals are measured for temperatures between 5 and 300 K and for eight different compositions. Structures in the $\rho(T)$ and $M(T)$ curves define characteristic temperatures which are used to construct a magnetic phase diagram. The large number of magnetic phases between ferromagnetic MnAs and antiferromagnetic CrAs are explained on the basis of two competing superexchange-double exchange magnetic couplings.

Das magnetische Moment M und der spezifische Widerstand ρ von $\text{Cr}_x\text{Mn}_{1-x}\text{As}$ -Polykristallen wird bei Temperaturen zwischen 5 und 300 K und für acht verschiedene Zusammensetzungen gemessen. Strukturen in den $\rho(T)$ - und $M(T)$ -Kurven definieren charakteristische Temperaturen die in einem magnetischen Phasendiagramm zusammengefaßt werden. Die große Zahl magnetischer Phasen zwischen ferromagnetischem MnAs und antiferromagnetischem CrAs wird auf zwei konkurrierende Superaustausch-Doppelaustausch-Kopplungen zurückgeführt.

1. Introduction

The electronic structure and the magnetic coupling in metallic transition metal compounds is not well understood as yet, in particular when a strong hybridization of the wave functions occurs together with strong correlations of the d-electrons [1, 2].

In this work a contribution to the problem of magnetic coupling has been made by investigating the transition from antiferromagnetic (afm) to ferromagnetic (fm) order for the 3d system CrAs-MnAs which also shows metallic conduction [2, 3].

The $\text{Cr}_x\text{Mn}_{1-x}\text{As}$ system was chosen since MnAs and CrAs are very similar in their properties, except for the magnetic order and form a completely miscible quasibinary alloy series [3 to 5]. Although there have been quite a few experimental investigations concerning this system [3 to 8] they have failed to give even the complete magnetic phase diagram as yet. By a combination of magnetic susceptibility and resistivity measurements we have completed the phase diagram. In the transitional region the magnetic behaviour is rather complex and unlikely to be explained by nearest-neighbour superexchange interactions or itinerant electron magnetism. An attempt is made to explain the transition in terms of the appearance of cation-valence fluctuations in the form of triangular resonant states with higher Mn contents.

2. Experimental

2.1 Preparation of the alloys

The $\text{Cr}_x\text{Mn}_{1-x}\text{As}$ alloys were prepared from the elements (Cr: 99.999%, Mn: 99.995% (Koch-Light Lab. Ltd.), As: 99.98% (Riedel de Haen AG)). The oxides of As were removed by sublimation. The powders were mixed (As in excess) and enclosed in a quartz ampoule at a pressure of 10^{-5} bar. Two different preparation techniques were used to obtain massive samples. The first method employs a closed iron tube to

¹⁾ Work supported by the Deutsche Forschungsgemeinschaft.

²⁾ Present address: Forschungslabor der AEG-Telefunken, Frankfurt, BRD.

protect the environment from an explosion of the ampoule when it is under high As pressure and is described in detail elsewhere [9]. The second method allowed to keep the As pressure p_{As} low and to vary it; this was done simply by varying the length of the ampoule in an oven with a given temperature profile [10]. After the temperature program (typical: 12 h 600 °C, 5 d 900 °C, 2 d 600 °C) was finished, the "hot" end of the ampoule contained the regulus while at the cool end the excess of As was deposited. By comparing the weights of (excess) As and regulus, we found that for p_{As} between 10^{-2} and 0.5 bar As is built into the crystal in the ratio 1:1 with an accuracy of 2×10^{-4} . Also, we did not find that a variation of p_{As} has any appreciable effect on the properties of the alloys. For low Cr or Mn contents, i.e. $x < 0.2$; $x > 0.8$ occasionally single crystal whiskers [9] were found on the polycrystalline material. They were used in some cases for the resistivity measurements $\rho(T)$. For the other compositions the regulus was remolten in a high-frequency oven using an inert atmosphere.³⁾ The composition of the samples which were used for the measurements was determined by means of the X-ray fluorescence of their solutions in aqua regia.⁴⁾ It was found that in all cases except one, the stoichiometry of the samples was confirmed within an accuracy of 2%.

2.2 Lattice parameters

The lattice parameters of the different compounds were obtained from X-ray diffraction of the polycrystalline powders (Debye-Scherrer method).⁵⁾ For all compositions the reflections were compatible with an orthorhombic MnP-type lattice (B31, space group D_{2h}^{16}). The sides a , b , c of the orthorhombic unit cell for different x are shown in

Table 1

Lattice constants and specific resistivity at 300 K for $Cr_xMn_{1-x}As$ compounds

| x | a_0 (Å) | b_0 (Å) | c_0 (Å) | $\rho_0 = \rho_{300\text{ K}}$ ($10^{-4} \Omega \text{ cm}$) |
|------------|-----------|-----------|-----------|---|
| CrAs (B31) | 5.643 | 3.455 | 6.203 | 9.1 |
| 0.8 | 5.655 | 3.533 | 6.210 | 58 |
| 0.7 | 5.665 | 3.540 | 6.215 | 17 |
| 0.5 | 5.660 | 3.588 | 6.243 | 8.2 |
| 0.4 | 5.666 | 3.578 | 6.255 | 11 |
| 0.31 | — | — | — | 7.9 |
| 0.2 | 5.675 | 3.590 | 6.280 | 19 |
| 0.1 | 5.703 | 3.596 | 6.298 | — |
| MnAs (B31) | 5.718 | 3.720 | 6.423 | 5.0 |

Table 1. The monotonous changes suggest that we have indeed a quasibinary alloy series without miscibility gaps except the one at $x = 0.07$ where an abrupt transition to the NiAs-type lattice (B8₁, space group D_{6h}^{47}) occurs for low temperatures. Also, for $1 \geq x > 0$ we never found diffraction patterns which could have indicated a two-phase region.

³⁾ Courtesy of Dr. H. Hohmann, Kristall-Labor SFB 126.

⁴⁾ Courtesy of Dr. H. J. Möller, Institut für Metallphysik, Universität Göttingen.

⁵⁾ Courtesy of Dipl. Phys. G. Daniel, Institut für Physikalische Chemie, Universität Göttingen.

2.3 Magnetization measurements

The magnetic moment M and the magnetic susceptibility χ were measured by the Faraday method as described elsewhere [11]. The accessible temperature range extended from 4 to 1000 K. However, in most cases the magnetic ordering temperatures were between room and nitrogen temperatures and M was recorded in just this range. Since for the ferromagnets of this system saturation could not be achieved at 1 T, for the magnetization versus temperature curves $M(T)$ the externally applied field B is given as a parameter. In those cases, where the magnetization versus field curves $M(B)$ were linear, χ is given in cgs units. In many cases the $M(T)$ curves for a fixed B showed irreversible changes with heating and cooling. However, generally after several cycles the material had stabilized; all the data presented are taken after stabilization.

2.4 Resistivity measurements

The $\rho(T)$ data were taken using a helium cryostat (Oxford CF 200) and alternating current (1 kHz) in connection with the four-point method. ρ -values taken at stationary conditions did not differ from those taken at a heating rate up to 3 K/min. In two cases ($x = 0.2$ and $x = 0.02$) we used small spiral single crystals with only two indium contacts attached for the $\rho(T)$ measurements. For $x = 0.2$ we could compare the result with the $\rho(T)$ curve of the polycrystalline specimen and found the same temperature dependence. This indicates that the spirals give a quasi-isotropic average and that it is possible to determine the composition of the whiskers from their characteristic transition temperatures. The latter were used to determine $x = 0.02$.

Within a heating-cooling cycle irreversible increases of $\rho(T)$ as large as 10% were observed with all polycrystalline samples. Since the same structures reappeared in the curves irrespective of cycle number we attribute the increases to microcracks which occur because of an interplay of thermal expansion and relaxation of internal strains. After several cycles the samples showed a tendency for stabilization. The data given represent the stabilized condition within 10%. However, since an unknown distribution of microcracks invalidates the determination of the absolute ρ -values from the geometrical dimensions and the resistance, the ρ -values at 300 K (ρ_0) as given in Table I can be wrong by a factor of two. Consequently, for the presentation of the temperature dependences $\rho(T)$ we have chosen a normalized scale $\rho/\rho_0 = \rho_r$.

The irreversible and hysteresis effects have no influence on the characteristic structures in $\rho(T)$ which reappear for all cycles indicating intrinsic effects. Also, some characteristic temperatures obtained this way coincide exactly with magnetic ordering temperatures [10] indicating that other characteristic temperatures supplement the ones from $M(T)$ and $\chi(T)$ measurements.

3. Results

3.1 $\chi(T)$ and $\rho(T)$ curves for $1 \geq x \geq 0.5$

Fig. 1 shows the susceptibility of $\text{Cr}_x\text{Mn}_{1-x}\text{As}$ crystals as a function of temperature $\chi(T)$. For CrAs the anomalous increase of χ above T_u is thought to be due to increasing ion displacements connected with the second-order $\text{B8}_1 \rightleftharpoons \text{B31}$ phase transition [1, 3, 5, 6] at $T_t = 831$ K. As with MnAs, the actual onset of magnetic order occurs simultaneously with a first-order transition of the lattice (T_u). In $\chi(T)$ we do not observe an abrupt step but a change of slope. In contrast to that, a CrAs single crystal whisker showed a discontinuity in $\rho(T)$ at T_N , as expected (Fig. 2a). Apparently, in $\chi(T)$ the discontinuity is smeared out because we have used a polycrystal. As may be inferred from the other $\chi(T)$ curves of Fig. 1 a fm order exists up to $x = 0.5$, but the transition

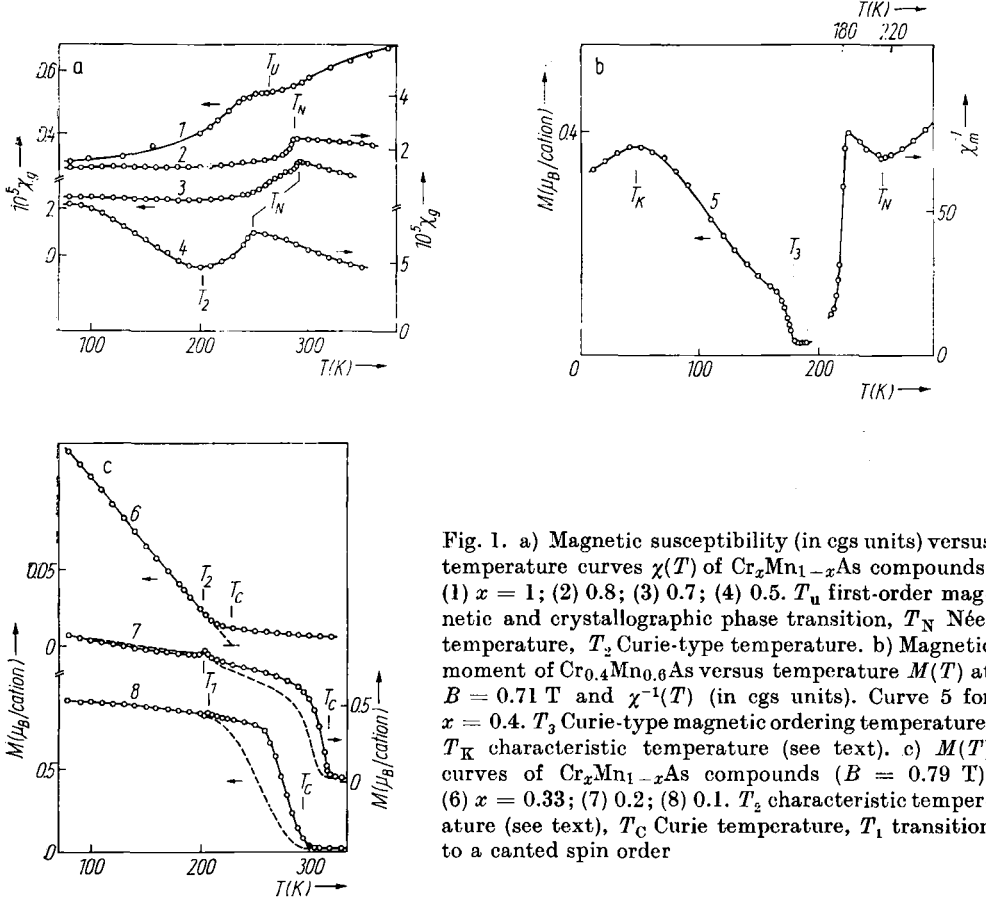


Fig. 1. a) Magnetic susceptibility (in cgs units) versus temperature curves $\chi(T)$ of $\text{Cr}_x\text{Mn}_{1-x}\text{As}$ compounds. (1) $x = 1$; (2) 0.8; (3) 0.7; (4) 0.5. T_u first-order magnetic and crystallographic phase transition, T_N Néel temperature, T_2 Curie-type temperature. b) Magnetic moment of $\text{Cr}_{0.4}\text{Mn}_{0.6}\text{As}$ versus temperature $M(T)$ at $B = 0.71 \text{ T}$ and $\chi^{-1}(T)$ (in cgs units). Curve 5 for $x = 0.4$. T_3 Curie-type magnetic ordering temperature, T_K characteristic temperature (see text). c) $M(T)$ curves of $\text{Cr}_x\text{Mn}_{1-x}\text{As}$ compounds ($B = 0.79 \text{ T}$). (6) $x = 0.33$; (7) 0.2; (8) 0.1. T_2 characteristic temperature (see text), T_C Curie temperature, T_1 transition to a canted spin order

changes its type; while for $x = 0.7$ we have observed a small-temperature hysteresis at T_N , for $x = 0.5$ the phase transition at T_N appears to be of the second kind. Also, for $x = 0.5$ a small ferromagnetic like rise appears at a lower temperature $T_2 < T_N$. A characteristic temperature near T_2 is also found in the $\rho(T)$ curve (Fig. 2a).

3.2 $M(T)$ and $\rho(T)$ curves for $x = 0.4$

For $x = 0.4$ (Fig. 1 b) a completely different kind of magnetism appears: the Néel point T_N is followed by a ferromagnetic rise which is nearly two orders of magnitude larger than the one for $x = 0.5$. The corresponding Curie-type ordering temperature is designated T_3 since from the $\rho(T)$ measurement another characteristic temperature T_2 with $T_3 < T_2 < T_N$ is identified (Fig. 2 b). The $\rho(T)$ anomaly is the same as for $x = 0.5$, but T_2 is different from the ferromagnetic rise for $x = 0.4$ (!). The ferromagnetic rise of $x = 0.4$ also shows a temperature hysteresis of $\approx 10 \text{ K}$ and drops again at low temperatures. We have characterized this drop by the temperature T_K of maximum magnetic moment. If T_K is defined this way it appears to be a function of applied field. A discontinuity near T_K is also found in the $\rho(T)$ curve. A similar behaviour is found in the system $\text{MnAs}_{1-x}\text{P}_x$ for $0.06 \leq x \leq 0.15$.

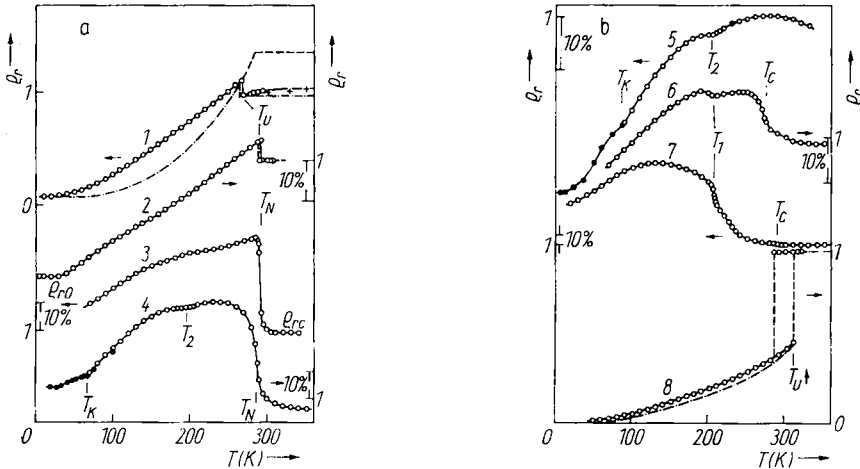


Fig. 2. a) Normalized resistivity $\rho_r = \rho/\rho_0$ versus temperature for $\text{Cr}_x\text{Mn}_{1-x}\text{As}$ compounds. (1) $x = 1$; (2) 0.8; (3) 0.7; (4) 0.5. +, ● data according to [3, 22], ρ_{r0} residual resistivity, ρ_{rc} resistivity in the paramagnetic state, - · - · - spin disorder scattering ρ_{sd} according to [21], - - - - ρ_{sd} extrapolated. b) $\rho_r(T)$ curves of $\text{Cr}_x\text{Mn}_{1-x}\text{As}$ compounds. (5) $x = 0.4$; (6) 0.31; (7) 0.2; (8) 0.02

3.3 $M(T)$ curve for $x = 0.33$

For increasing Mn content ($x < 0.4$) one would expect that the tendency for ferromagnetism increases. However, this is not the case as may be seen from Fig. 1c ($x = 0.33$). The absolute values of M for a given B are lower as compared to $x = 0.4$ and the nearly linear rise of $M(T)$ is rather unusual. It allows the definition of a magnetic ordering temperature T_C by its intercept with the T -axis. In the scale used in Fig. 1c a little hump which shows in $M(T)$ at $T_2 < T_C$ is not resolved; it is clearly present in an enlarged scale. Also, $T_1 \approx T_2$ shows as a characteristic structure in $\rho(T)$ of $x = 0.31$ (Fig. 2b).

3.4 $M(T)$ and $\rho(T)$ for $0.3 \geq x \geq 0.1$

The $M(T)$ curves for $x = 0.2$ and $x = 0.1$ are similar and show definitely a ferromagnetic behaviour (T_C 's in Fig. 1c). Curiously, there is a little Néel-point-like hump (T_1) sitting on the part of the $M(T)$ curve which corresponds to ferromagnetic order in both cases. From the small drop of $M(T)$ for $T \lesssim T_1$ one is led to assume that the spin arrangement below T_1 has a smaller ferromagnetic component than that for $T > T_1$.

The $M(T)$ curve for still higher Mn contents ($x < 0.07$) resembles that of MnAs [13].

3.5 Phase transition temperatures

All the characteristic temperatures which are identified from the $\rho(T)$ and $M(T)$ curves are summarized in the magnetic phase diagram (Fig. 3). Since the effects of magnetic order on ρ and M are quite different, in some cases a specific ordering temperature is resolved in $\rho(T)$, but not in $M(T)$ and vice versa. Also, in some cases we have observed shifts in some magnetic ordering temperatures when the material was remelted for the resistivity measurements. This is assigned to the strain sensitivity of some magnetic parameters. Consequently, samples which showed too large shifts in respect to the original (annealed) material, were not considered.

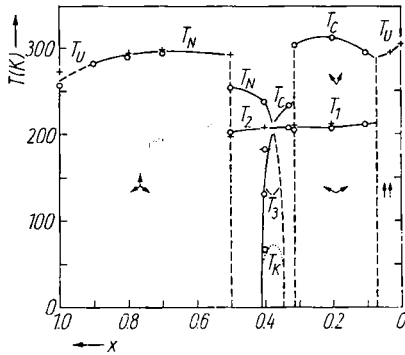


Fig. 3

Fig. 3. Magnetic phase diagram of the $\text{Cr}_x\text{Mn}_{1-x}\text{As}$ system. Spin arrangements as shown are schematic

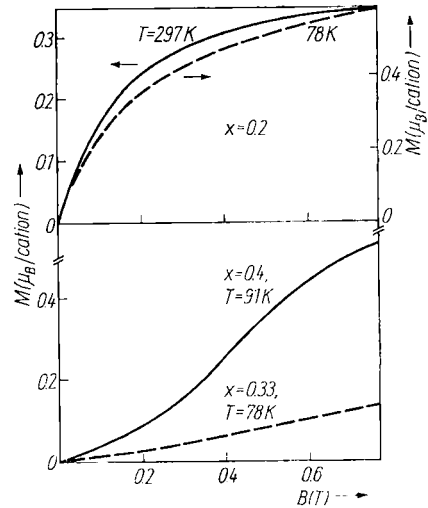


Fig. 4

Fig. 4. Magnetization versus external field curves $M(B)$ of $\text{Cr}_{0.2}\text{Mn}_{0.8}\text{As}$ for two different temperatures ($T = 297\text{ K}$; $T = 78\text{ K}$) and $M(B)$ of $\text{Cr}_{0.4}\text{Mn}_{0.6}\text{As}$ and $\text{Cr}_{0.33}\text{Mn}_{0.67}\text{As}$ at nearly the same temperature ($T = 91\text{ K}$; $T = 78\text{ K}$)

Aside from constructing the phase separation lines by connecting the characteristic temperatures, $M(B)$ curves at different temperatures served as a valuable supplement for the identification of the different phase regions. Note, for example, that the $M(B)$ curves for $x = 0.2$ at $T = 297\text{ K}$ and $T = 78\text{ K}$ (Fig. 4) are different in shape: while for each external field value B the magnetic moment is higher for $T = 78\text{ K}$, as it should be when less spin waves are excited, the material evidently is harder to saturate. Since $78\text{ K} < T_1 < 297\text{ K}$, this is assigned to the different spin order above and below T_1 . Equally, when we find qualitatively different $M(B)$ curves at the same temperature for two different compositions x_1, x_2 , we will have to suspect a phase separation line in between. Fig. 4 shows $M(B)$ for $x_1 = 0.4$ and $x_2 = 0.33$ at nearly the same temperature. Note that when we draw a phase separation line according to the gross differences in the $M(B)$ curves (Fig. 3; dashed line) the magnetic phase diagram obtains a symmetric form for $0.5 > x > 0.32$. This in turn defines an existence region for a magnetic phase γ , an example of which is given by Fig. 1 b ($x = 0.4$); then, from the existence of $T_K(B)$ another phase separation line suggests itself. We have drawn the (dotted) line $T_K(0.3\text{ T})$ so that it is restricted to the existence region of γ .

4. Discussion

4.1 Compensated spin arrangements for $1 \geq x \geq 0.5$

4.1.1 First-order phase transition and magnetic coupling in CrAs

The nature of the magnetic and crystallographic transitions in CrAs has attracted some attention [3, 5 to 7, 12]. As CrAs has the same sequence of phase transitions ($T_t > T_u$) as MnAs we propose that this is a consequence of an interplay of the energies and

entropies of a soft phonon mode and an ordering spin system [14]. Also, with the static ion displacements ("orthorhombic distortion") following the displacive phase transition at T_t the $p_\pi e_2$ hybridization changes significantly and yields a high-spin (hs)-low-spin (ls) transition simultaneously with a dramatic change in the magnetic coupling [1]. Both effects superimpose and lead to the anomalous part of the $\chi(T)$ curve ($T_u < T < T_t$) [1]. However, since for CrAs $S \approx 1$ [3] below T_u , which is intermediate between the ls ($S = \frac{1}{2}$) and the hs ($S = \frac{3}{2}$) value, the hs-ls transition is incomplete. In the high temperature hexagonal ($B8_1$) phase Cr^{3+} would have $(e_2)^2 (a_1)^1$ as high spin or $(e_2)^3$ as low spin pure crystal field state. From $S \approx 1$ it follows that some a_1 electron states are occupied. Since the a_1 -orbitals are directed along c and always overlap strongly they form a quasi-one-dimensional band which has a strong tendency to split with the introduction of a superlattice along c . Since an orthorhombic distortion already doubles the periodicity along c , it is suggestive to assume that below T_u the a_1 -band is split into empty and full subbands because of both distortion and antiferromagnetic order [2]. Since the a_1 -states can only be occupied at the expense of spin-down e_2 -states this would mean $S = 1$ per cation, which corresponds well to the measured permanent magnetic moment per cation $p_{\text{Cr}} = 2\mu_B$ (neutron diffraction). With a split a_1 -subband, the a_1 -electrons can be considered fairly localized again and the magnetic coupling comes from a_1 - p_π - a_1 and e_2 - p_π - e_2 superexchange contributions which are both negative. Although there have been attempts to explain the helimagnetism of CrAs in terms of anisotropic superexchange and additional next-nearest-neighbour interactions [8] the helical ordering could also indicate additional double exchange effects and next-nearest-neighbour interactions [15].

4.1.2 Magnetic coupling in $\text{Cr}_{0.5}\text{Mn}_{0.5}\text{As}$

The magnetic coupling of $\text{Cr}_{0.5}\text{Mn}_{0.5}\text{As}$ can be discussed in terms of localized pure crystal field states, whereby the orthorhombic distortion is neglected. Adding ls Mn: $(e_2)^3 (a_1)^1$ to low-spin Cr: $(e_2)^3$ would serve to fill the Cr a_1 -states at the expense of the Mn a_1 -states. Again, at $x = 0.5$ the joint quasi-one-dimensional a_1 -band would be exactly half-filled. In this case the introduction of afm order at T_N alone suffices to split the a_1 -band; there is no need for the orthorhombic distortion to be enhanced in a first-order transition and $S = 1$. Actually, $p_a(x = 0.7) = 2.1\mu_B$ and the transition is of the second kind.

The splitting of the a_1 -subband is confirmed by the $\varrho(T)$ curves: for $x = 0.5$ the $\varrho(T)$ increase (!) on cooling at T_N is even stronger [10] than the one observed for $x = 0.7$ (Fig. 2). For the magnetic coupling we have again negative e_2 - p_π - e_2 and a_1 - p_π - a_1 contributions. Adding more Mn would mean a filling of the split-off a_1 -subband before (extended) e_1 -states (which have been considered empty so far) can possibly be occupied; the latter would correspond to adding high-spin Mn atoms: $(e_2)^1 \times (a_1)^1 (e_1)^1$; $S = 2$.

4.2 Percolation of cation triangles

4.2.1 Double exchange effects for $x < 0.32$

The $M(T)$ and $M(H)$ curves for $0.08 < x < 0.32$ indicate the existence of fm double-exchange mechanisms which are superimposed to afm superexchange and dominate it: $T_C > T_1$ (T_1 transition to a canted spin order) [15]. However, since double exchange is conventionally connected with resonant electron transfer between mixed valency pairs [16] and if Mn and Cr would have different valences, ferromagnetism connected with an infinite cluster of Cr-Mn pairs should set in at $x \approx 0.85$ already [17]. The fact that fm appears when the ratio of Mn: Cr is near 2:1 indicates that a larger reso-

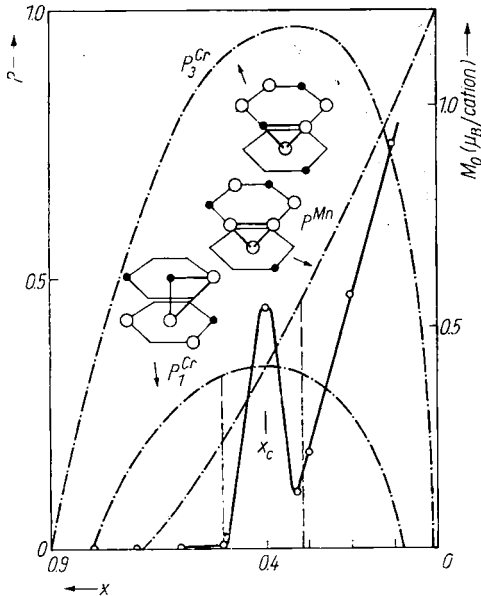


Fig. 5. Percolation probabilities for the formation of infinite clusters of Mn-Mn-Mn (P^{Mn}) triangles and two types of Mn-Mn-Cr triangles (P_3^{Cr} , P_1^{Cr}) and magnetic moment M_0 at $T = 80$ K and $B = 0.8$ T as a function of Cr content x . x_c characteristic concentration where $P_1^{\text{Cr}} = P^{\text{Mn}}$ (for more details see text). \circ Mn, \bullet Cr

nant unit forms an infinite cluster. Since for manganese pnictides double-exchange coupling has been assigned to free triangular resonant states [1], whereby an electron-hole pair rotates, giving the same average valence at each cation site, we have investigated the probability for Mn-Mn-Mn and Cr-Mn-Mn triangles to form infinite clusters. Fig. 5 shows the percolation probabilities $P^{\text{Mn}}(x)$, $P_3^{\text{Cr}}(x)$, and $P_1^{\text{Cr}}(x)$ for a Bethe lattice

made of triangles as shown in [18]; the coordination number reproduces the local structure of the real (B8_1) lattice. P should scale with the magnetization M_0 at $T = 0$. Note that $M_0(x)$ is not symmetric as it would be if Cr-Mn pairs or Cr-Mn-Mn triangles were involved. This strongly favours an interpretation of the onset of ferromagnetism in terms of Mn-Mn-Mn resonant units although $M_0(x)$ appears to be shifted in respect to P^{Mn} ; this shift is certainly not due to the fact that the Bethe calculation is only asymptotically exact for high coordination numbers, but rather indicates that P^{Mn} has to be folded with the occupation number $N_r^{\text{Mn}}(x)$ of the resonant states. $N_r^{\text{Mn}}(x)$ is not a constant and should resemble a step function at $x = 0.5$: if one has a free $(p_\pi e_2)^3 - (p_\pi e_1)^3$ resonance [1] to move inside the Mn-Mn-Mn cluster, for the occupation of its states e_1 electrons are necessary. From the discussion in Section 4.1.2 we cannot expect e_1 transfer electrons for $1 > x > 0.5$.

4.2.2 Double-exchange effects for $0.5 \geq x \geq 0.32$

If one accepts the interpretation given in Section 4.2.1 the fm precursor in the $M_0(x)$ curve and the complexity of the magnetic phase diagram between $x = 0.5$ and $x = 0.32$ suggest that apart from the Mn-Mn-Mn mechanism (B) at least one additional mechanism (A) is present. According to the $M(T)$ curves for $x = 0.5$ and $x = 0.4$ (Fig. 1 a, b) we have to suspect again an fm DE mechanism which is superimposed to afm superexchange. For its identification we resort to the calculation of percolation probabilities as before. The percolation probability of Mn-Mn-Cr triangles P_3^{Cr} can be ruled out since it is symmetric and would exceed P^{Mn} everywhere except for $x < 0.12$. In contrast to that, the percolation of Mn-Mn-Cr triangles involving a_1 -states, P_1^{Cr} , has a comparable probability in a compositional region which more closely coincides with $0.5 \geq x \geq 0.32$. While the cut-off at $x = 0.5$ could be assigned to a step function of $N_1^{\text{Cr}}(x)$ as before, for $x \leq 0.3$ $2P_1^{\text{Cr}} \leq P^{\text{Mn}}$ and it would be not too surprising if the magnetic behaviour were dominated by the B-type of coupling only. For the remaining region we would expect a mixed magnetic state; however, even if P_1^{Cr}

couples afm a complete miscibility can be ruled out since it would not account for the maximum of $M_0(x)$. This ferromagnetic precursor is interpreted as an “intermagnetic” compound, i.e. a joint percolation of type A and B resonances when they are present in a certain ratio. Then, the correct choice of the second DE-SF mechanism, P_1^{Cr} , is most convincingly demonstrated by the coincidence of $x_c = 0.385$ (where $P^{\text{Mn}} = P_1^{\text{Cr}}$) with the “hexuple” point of the magnetic phase diagram (cf. Section 4.2.3).

4.2.3 *Mixing of two kinds of magnetic couplings*

If, according to Section 4.2.2 one considers the magnetism of $\text{Cr}_{0.4}\text{Mn}_{0.6}\text{As}$ as due to an interplay of two types of triangular resonances, for the whole region $0.5 \geq x \geq 0.32$, since there is a comparable probability for both types to extend through the lattice, the majority of cations will belong simultaneously to a Mn-Mn-Cr (A) and a Mn-Mn-Mn (B) triangle and it is suggestive to consider the magnetic phases as a result of a mixing of the two types of resonant configurations. If one neglects the excitations of the spin system and decomposes the total free energy of the system into a sum of the free energies F_i of the pure constituents and a mixing term F^M [19], i.e.

$$F = \sum_{i=1}^2 n_i F_i + F^M, \tag{1}$$

where $n_{1,2}$ relative numbers of triangles A, B per cm^3 , one can derive the mixing free-energy part F^M analogous to binary alloys where the phonon modes are neglected in a first approximation. In what follows F^M will be calculated for a simplified configurational model (Fig. 6a); however, it is assumed that the result can be generalized. In Fig. 6a a network of Mn-Mn-Mn (B) triangles establishes planes which are linked by Mn-Mn-Cr (A) triangles. While the picture as drawn corresponds to a compound with the ratio of triangles $N_B:N_A = 3:2$, the ratio of Mn:Cr = 3:2 and $x = 0.4$, for a small deviation from $x = 0.4$ most of the Mn atoms (N_0) will still be linked to both types of triangles. Certainly, for larger deviations

the one or the other type will percolate and eventually introduce a more or less well defined cut-off composition at each side ($x_{1,2}^c$). For the remaining range, if we have one (or less) transfer electron per Mn atom, we cannot possibly occupy all $(N_0 + \frac{2}{3}N_0)$ triangular resonant states (A, B). In order to obtain the mixing entropy we now have to calculate the possibilities to distribute the electrons onto the triangles. For an approximate result we ignore the excess of B-triangles, i.e. $N_A = N_B = N_0$ for $x = 0.4$ and assume that a deviation from $x = 0.4$ enhances N_A and decreases N_B (and vice versa) such that $N_A + N_B = 2N_0 = \text{const.}$ Then, if we have one

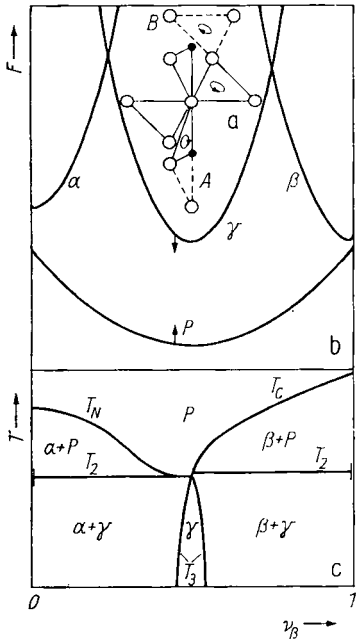


Fig. 6. Free energy F versus concentration of triangles ν_A, ν_B for different magnetic phases in a mixing model and magnetic phase diagram obtained using the double tangent construction; parabolas α, β remain fixed while parabolas γ, P shift linearly downward (upward) with temperature (they meet in highly symmetrical configuration)

electron per Mn atom and introduce molar fractions with $\nu_A + \nu_B = 1$,

$$N_a = N_0 \nu_A(x) \quad \text{and} \quad N_b = N_0 \nu_B(x) \quad (2)$$

are the numbers of occupied resonances (for $x = 0.4$, $\nu_A = 0.5 = \nu_B$). The number of possibilities to distribute $N_0 \nu_A$ ($N_0 \nu_B$) electrons onto N_0 triangles is

$$w = \frac{N_0!}{(N_0 \nu_A)! (N_0 \nu_B)!} \quad (3)$$

Use of the Boltzmann definition of the entropy yields the well-known result

$$S = -2N_0 k (\nu_A \ln \nu_A + \nu_B \ln \nu_B) \quad (4)$$

Continuing the analogy the mixing energy E^M can be expressed in terms of the relative numbers of pairs AA, AB, BB of triangles with double exchange plus superexchange energies ε_{AA} , ε_{AB} , ε_{BB} . The total internal energy E we obtain from the summation over all pairs

$$E = \frac{1}{2N_0} (z_{AA} P^{AA} \nu_A \varepsilon_{AA} + z_{AB} P^{AB} \nu_A \varepsilon_{AB} + z_{BA} P^{BA} \nu_B \varepsilon_{BA} + z_{BB} P^{BB} \nu_B \varepsilon_{BB}), \quad (5)$$

whereby P^{AA} , ... are the probabilities to find an A-resonance neighbouring an A-resonance, and z_{AA} , ..., the coordination numbers for the triangles. If we ignore the differences in z_{AA} , ..., such that the probabilities observe the sum rules, we recover

$$E = E_0 + E^M = \frac{1}{2N_0} \bar{z} (\nu_A \varepsilon_{AA} + \nu_B \varepsilon_{BB}) + N_0 z \nu_A P^{AB} \varepsilon \quad (6)$$

with $\varepsilon = \varepsilon_{AB} - \frac{1}{2}(\varepsilon_{AA} + \varepsilon_{BB})$ as "replacement energy" and $\bar{z} (\approx 4)$ as an average coordination number. If there is a statistical distribution of the electrons on A and B triangles at high temperatures, $P^{AB} \approx \nu_B$ and the final result is

$$F^M = E^M - T S^M = N_0 \bar{z} \nu_A \nu_B \varepsilon + 2N_0 k T (\nu_A \ln \nu_A + \nu_B \ln \nu_B). \quad (7)$$

As with binary alloys, the use of (7) together with the stability conditions (double tangent rule) yields a variety of different phase diagrams depending on the choice of the replacement energy ε , which also provides a basis for the existence of "intermetallic compounds".

We have tried to reconstruct the experimentally observed phase diagram for $0.5 \geq x \geq 0.32$ using parabolic free-energy curves which shift with temperature (Fig. 6 b, c). In particular, we have assumed an extremely small miscibility in the magnetically ordered phase and the existence of an "intermetallic" compound $A_m B_n$ (γ -phase). This approach defines T_2 as an eutectic line and T_3 as the boundaries of the existence region of $A_m B_n$. If $x_1 = 0.5$ were the α -phase and $x_2 = 0.32$ the β -phase, $m:n$ would be 2:3; however, since $x_{1,2}$ presumably are cut-off compositions, the ratio could be different. The proposed existence of an "intermagnetic" compound corresponds well to the unexpectedly strong ferromagnetism of the γ -phase as compared to neighbouring compositions and to the characteristic sequence of magnetic ordering in $\text{Cr}_{0.4}\text{Mn}_{0.6}\text{As}$ [3, 4], including the low-temperature anomaly at T_K which might indicate a low-temperature condensation phenomenon of the double-exchange electrons (holes) [20].

While the model can account for all the experimentally observed phase transition lines, the region where paramagnetism and antiferromagnetism (or pm and DE-SE ferromagnetism) shall coexist certainly is an artifact resulting from the omission of the excitations of the spin system. Since for the pure constituents (α , β phases) the molecular field calculation of de Gennes [15] can be used we expect two magnetic

ordering temperatures $T_N > T_1$ (or $T_C > T_1$) separating a pm, afm(fm), and a canted magnetic phase region not only for the α, β, γ phases but also for the intermediate region. Although the de Gennes model provides a physically plausible correction of the mixing model (the pm/afm region is really afm with fm fluctuations, etc.) it cannot be used to replace it since it would not account for the "eutectic" line T_2 .

4.3 Specific resistivity

As the approach used to explain the magnetic phase diagram mixes two kinds of free excitons, a metallic conductivity seems to be ruled out. However, given a partial thermal decomposition of the electron-hole pairs, free carriers exist which can scatter on the (residual) localized spins. Since this situation resembles sd scattering it can be understood why at T_2 $\rho(T)$ shows a distinct dip: since the fm fluctuations disappear below T_2 we expect a reduction in the spin disorder scattering [21, 23]. The existence of a spin disorder scattering mechanism itself appears to be justified from its successful application to the resistivity of MnAs and CrAs (Fig. 2a, b). Note that for CrAs one has to consider a step in ρ due to the splitting of the a_1 -subband at T_u in addition. This effect should also occur when we increase the antiferromagnetic component at T_1 or when a canted spin order is introduced at T_C . The $\rho(T)$ anomaly at T_K is assigned to the type of low-temperature scattering mechanism which has been identified for $\text{MnAs}_{1-x}\text{P}_x$ compounds [20]. However, even for compounds without T_K we find an extremely large residual resistance when $1 > x > 0.02$. This is most likely connected with the random cation mixture which gives rise to large spin-dependent and spin-independent scattering potentials [24, 25].

Acknowledgements

The authors would like to thank Prof. Dr. H.-U. Harten for valuable support, and Dr. L. Turban for valuable discussions.

References

- [1] K. BÄRNER, *phys. stat. sol. (b)* **88**, 13 (1978).
- [2] K. BÄRNER, *phys. stat. sol. (b)* **84**, 385 (1977).
- [3] N. KAZAMA and H. WATANABE, *J. Phys. Soc. Japan* **30**, 1319 (1971).
- [4] H. WATANABE, N. KAZAMA, Y. YAMAGUCHI, and M. OHASHI, *J. appl. Phys.* **40**, 1128 (1969).
- [5] H. IDO, *J. Phys. Soc. Japan* **27**, 318 (1969).
- [6] H. BOLLER and A. KALLEL, *Solid State Commun.* **9**, 1699 (1971).
- [7] K. SELTE, A. KJEKSHUS, W. E. JAMISON, A. F. ANDRESEN, and J. E. ENGBRETSSEN, *Acta chem. Scand.* **25**, 1703 (1971).
- [8] A. KALLEL, H. BOLLER, and E. F. BERTAUT, *J. Phys. Chem. Solids* **35**, 1139 (1974).
- [9] K. BÄRNER, *Phys. Letters A* **35**, 333 (1971).
- [10] R. WÖHL, Diploma Work, Göttingen 1978.
- [11] H. BERG, *phys. stat. sol. (a)* **40**, 559 (1977).
- [12] M. YUZURI, *J. Phys. Soc. Japan* **15**, 2007 (1960).
- [13] K. BÄRNER, *phys. stat. sol. (a)* **5**, 405 (1971).
- [14] K. BÄRNER and H. BERG, *phys. stat. sol. (a)* **49**, 545 (1978).
- [15] P. G. DE GENNES, *Phys. Rev.* **118**, 141 (1960).
- [16] P. W. ANDERSON and H. HASEGAWA, *Phys. Rev.* **100**, 675 (1955).
- [17] J. B. GOODENOUGH, *Magnetism and the Chemical Bond*, Wiley, New York/London 1963 (p. 229).
- [18] L. TURBAN, private communication, 1979.
- [19] P. HAASEN, *Physikalische Metallkunde*, Springer-Verlag, Berlin/New York 1974 (p. 85).

- [20] H. BERG and K. BÄRNER, *J. Magnetism magnetic Mater.* **4**, 69 (1977).
- [21] T. KASUYA, *Progr. theor. Phys. (Kyoto)* **16**, 58 (1956).
- [22] H. J. KROKOSZINSKI, private communication, 1979.
- [23] K. KUBO and N. OHATA, *J. Phys. Soc. Japan* **33**, 21 (1972).
- [24] A. J. DECKER, *J. appl. Phys.* **36**, 906 (1965).
- [25] E. GRATZ and C. A. POLDY, *phys. stat. sol. (b)* **82**, 159 (1977).

(Received November 5, 1979)